



ELSEVIER

Available online at www.sciencedirect.com



Catalysis Today xxx (2007) xxx–xxx



www.elsevier.com/locate/cattod

A combined solar photocatalytic-biological field system for the mineralization of an industrial pollutant at pilot scale

I. Oller^a, S. Malato^{a,**}, J.A. Sánchez-Pérez^b, W. Gemjak^a, M.I. Maldonado^a,
L.A. Pérez-Estrada^a, C. Pulgarín^{c,*}

^a *Plataforma Solar de Almería (CIEMAT), Carretera Senés, Km 4, 04200 Tabernas (Almería), Spain*

^b *Departamento de Ingeniería Química, Universidad de Almería, Crta de Sacramento s/n, 04120 Almería, Spain*

^c *Ecole Polytechnique Fédérale de Lausanne, Institute of Chemical Sciences and Engineering, GGEC, Station 6, CH-1015 Lausanne, Switzerland*

Abstract

A coupled solar photocatalytic-biological pilot plant system has been employed to enhance the biodegradability and complete mineralization of a biorecalcitrant industrial compound, α -methylphenylglycine, dissolved in distilled water and simulated seawater at 500 mg L⁻¹. The pollutant was completely degraded by a solar photo-Fenton treatment in a 75-L pilot plant made up of four compound parabolic collector (CPC) units. The catalyst concentration employed was 2 and 20 mg L⁻¹ of Fe²⁺ and the H₂O₂ concentration was kept in the range of 200–500 mg L⁻¹. A Zahn–Wellens (Z–W) test applied to photo-treated samples demonstrated that intermediates produced within a short time of starting the photo-Fenton process were biodegradable. Consequently, the photocatalytic and biological processes were combined. Biodegradable compounds generated during the preliminary oxidative process were biologically mineralized in a 170-L aerobic immobilised biomass reactor (IBR), filled with 90–95 L propylene Pall Ring supports colonized by activated sludge. Almost total mineralization (90% overall total organic carbon removed) was attained in the combined treatment system (for both distilled and seawater experiments). Moreover, nitrification and denitrification phenomena were also observed.

© 2007 Published by Elsevier B.V.

Keywords: Photocatalysis; Photo-Fenton; Immobilised biomass reactor; α -Methylphenylglycine; Biodegradability; Nitrification; Denitrification

1. Introduction

Industrial waste water containing toxic and/or non-biodegradable organic pollutants are not treatable by conventional biological processes. Although biological treatment is often the most cost-effective alternative it is often not effective for industrial effluents contaminated with biorecalcitrant organic substances.

The high potential and effectiveness of Advanced Oxidation Processes (AOPs) for the total oxidation of hazardous organic compounds is widely recognized [1,2]. AOPs are characterized by the production of hydroxyl radicals (\cdot OH), the second strongest known oxidant after fluorine. This hydroxyl radical attacks organic molecules, yielding carbon dioxide, inorganic

ions and water. The advantage of AOPs is enhanced by the fact that \cdot OH radicals may be produced in different ways, so they can be adapted to specific treatment requirements.

Among the AOPs, the photo-Fenton system [3], has been shown to be the most promising for the remediation of contaminated water [4]. Moreover, as UV radiation generation by lamps or ozone production is expensive, photo-Fenton driven by solar radiation is of special interest, making the development of suitable technologies very attractive for practical applications [5–6].

The major drawback of AOPs is that their operating costs exceed those of biological treatment. Nevertheless, the use of AOPs as a pre-treatment step to enhance the biodegradability of waste water containing recalcitrant or inhibitory pollutants can be justified if the resulting intermediates are easily degradable by micro-organisms in further biological treatment.

Many reports have focused on the study of new chemical-oxidation technologies as a pre-treatment for non-biodegradable or toxic waste water combined with a conventional biological treatment [7–9]. These results, mainly from laboratory studies,

* Corresponding author. Tel.: +41 21 693 4720; fax: +41 21 6934722.

** Corresponding author. Tel.: +34 950 387940; fax: +34 950 365015.

E-mail addresses: sixto.malato@psa.es (S. Malato), cesar.pulgarin@epfl.ch (C. Pulgarín).

61 suggest potential advantages for water treatment. Recently, very
62 attractive combined systems have been proposed to treat
63 different kinds of industrial waste water [10–16].

64 Today combined photo-assisted AOP and biological processes
65 are gaining in importance as treatment systems, as one of
66 the main urban waste water treatment obligations imposed by
67 European Union Council Directive 91/271/EEC is that waste
68 water collecting and treatment systems (generally involving
69 biological treatment), must be in place in all agglomerations of
70 between 2000 and 10,000 population equivalents by 31st
71 December 2005. Smaller agglomerations which already have
72 a collecting system must also have an appropriate treatment
73 system by the same date [17]. In a near future, AOP plants
74 developed in the EU could be discharging pre-treated waste
75 water into a nearby conventional biological treatment plant.

76 This work evaluates the feasibility of coupling a photo-
77 reactor with to a biological field system at pilot scale employing
78 photo-Fenton pre-treatment of a biorecalcitrant industrial
79 compound, α -methylphenylglycine (MPG), dissolved in distilled
80 water and simulated seawater. These two extreme
81 situations are compared, as the photo-Fenton reaction rate in
82 waste water containing typical freshwater inorganic species (in
83 the range of mM units), is usually almost the same as in
84 demineralized water. It should be remarked that a pH between
85 2.8 and 2.9 (optimal for photo-Fenton treatment) avoids the
86 presence of inorganic carbon species, which are purged as CO_2
87 during pH adjustment of the waste water. A different situation
88 arises in the presence of large quantities of sodium chloride
89 (i.e., seawater), when photo-Fenton very often is not able to
90 substantially mineralize the organic content of the waste water
91 [18,19].

92 MPG, a common precursor in pharmaceuticals, was selected
93 because of its non-biodegradability and high water solubility.
94 Degradation and mineralization (TOC disappearance) of the
95 parent compound were analysed, and nitrification and denitrification
96 phenomena were also observed. Experiments in chemical and biological
97 characterisation of photo-treated solutions were performed in order
98 to establish when the photo-treated solution becomes biocompatible.
99 The biological system (immobilised biomass reactor) which completes
100 the photo-chemical pre-treatment should be compact, modular, flexible
101 and resistant to toxic shock, and variations in charge and flow.

102 2. Experimental

103 2.1. Chemicals

104 Technical-grade MPG (α -methylphenylglycine, $\text{C}_9\text{H}_{11}\text{NO}_2$)
105 was used as received (Diagram 1). The initial concentration
106 in all experiments was 530 mg L^{-1} . MPG tests were performed
107 using distilled water from the Plataforma Solar de Almería (PSA)
108 distillation plant (conductivity $< 10 \mu\text{S cm}^{-1}$, $\text{Cl}^- = 0.7\text{--}0.8 \text{ mg L}^{-1}$,
109 $\text{NO}_3^- = 0.5 \text{ mg L}^{-1}$, organic carbon $< 0.5 \text{ mg L}^{-1}$), and
110 simulated seawater prepared with 35 g L^{-1} of NaCl (reagent grade,
111 Panreac). Photo-Fenton experiments were performed using iron
112 sulphate ($\text{FeSO}_4 \cdot 7\text{H}_2\text{O}$), reagent grade hydrogen peroxide
113 (30%, w/v) and sulphuric acid for pH

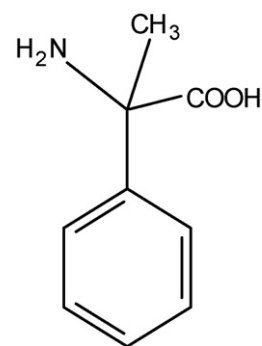


Diagram 1. Chemical structure of α -methylphenylglycine (MPG).

114 adjustment (around 2.7–2.9), all provided by Panreac. The
115 photo-treated solutions were neutralised by means of NaOH
116 (reagent grade, Panreac). Neutral pH of the solutions was
117 maintained during the biological treatment by adjusting with
118 H_2SO_4 (reagent grade, Panreac) and NaOH. The nutrient salts
119 used in the biological reactor (P, N, K and oligoelements) were
120 added from standard solutions (Panreac).

121 2.2. Analytical determinations

122 MPG concentration was analysed using reverse-phase liquid
123 chromatography (flow 0.5 mL min^{-1}) with a UV detector in
124 an HPLC-UV (Agilent Technologies, series 1100) with C-18
125 column (LUNA $5 \mu\text{m}$, $3 \text{ mm} \times 150 \text{ mm}$ from Phenomenex).
126 Ultra pure distilled-deionised water obtained from a Milli-Q
127 (Millipore Co.) system and HPLC-graded organic solvents
128 were used to prepare all the solutions. The mobile phase
129 composition employed for detecting the pollutant was phosphoric
130 acid at 50 mM adjusted to pH 2.5 with NaOH, at a
131 wavelength of 210 nm .

132 Mineralization was monitored by measuring the total
133 organic carbon (TOC) by direct injection of filtered samples
134 into a Shimadzu-5050A TOC analyser provided with a NDIR
135 detector and calibrated with standard solutions of potassium
136 phthalate.

137 Ammonium concentration was determined with a Dionex
138 DX-120 ion chromatograph equipped with a Dionex Ionpac
139 CS12A $4 \text{ mm} \times 250 \text{ mm}$ column. Isocratic elution was done
140 with H_2SO_4 (10 mM) at a flow rate of 1.2 mL min^{-1} . NH_4^+
141 was measured in simulated saline samples using the Colorimetric
142 Phenate Method (American Standard Methods, no. 4500).
143 Anion concentrations (NO_3^- and NO_2^-) were determined with
144 a Dionex DX-600 ion chromatograph using a Dionex Ionpac
145 AS11-HC $4 \text{ mm} \times 250 \text{ mm}$ column. The gradient programme
146 was pre-run for 5 min with 20 mM NaOH, an 8-min injection of
147 20 mM of NaOH, and 7-min with 35 mM of NaOH, at a flow
148 rate of 1.5 mL min^{-1} .

149 Colorimetric determination of total iron concentration with
150 1,10-phenantroline was used following ISO 6332. Hydrogen
151 peroxide analysis was carried out by iodometric titration,
152 although, since this method is very time consuming (around
153 45 min), it was frequently determined in fresh sample solutions
154 using Merckoquant Paper (Merck Cat. No. 1.10011.0001) just
155

to get an idea of overall H_2O_2 consumption and to detect any significant decrease.

2.3. Biodegradability assays

An adaptation of the EC protocol (Directive 88/303/EEC) was followed to determine the biocompatibility of the pre-treated MPG waste water at different stages of photo-Fenton process. This method, called the Zahn–Wellens test (Z–W), is used to evaluate the biodegradability of water-soluble, non-volatile organic contaminants when exposed to relatively high concentrations of micro-organisms. Activated sludge from the Waste water Treatment Plant in Almería (AQUALIA), mineral nutrients and test material as the sole carbon source are placed together in a 0.25-L glass vessel equipped with an agitator and aerator. The test lasts around 28 days and is kept at 20–25 °C under diffuse illumination (or in a dark room). The blank is prepared using distilled water instead of test water, mineral nutrients and an amount of bacteria representative of the inoculum present in the test solutions. A vessel containing diethylene glycol, a well-known biodegradable substance recommended by the protocol mentioned above is run in parallel in order to check the activity of the activated sludge. Degradation is monitored by DOC determination in the filtered solution (with the TOC analyser), daily or at other appropriate regular time intervals. The initial DOC is always determined 3 h after test start-up in order to detect adsorption of contaminants by the activated sludge. Loss of volume from evaporation (due to agitation and aeration) is adjusted before each sampling with distilled water in the required amounts. The ratio of eliminated DOC after each interval to the initial DOC is expressed as the percentage of biodegradability: $100 [1 - (C_t - C_B / C_A - C_{BA})]$. C_A is the DOC (mg/L) in the test mixture, measured 3 h after the beginning of the test, C_t the DOC at time t , C_B the DOC of the blank at time t and C_{BA} is the DOC of the blank 3 h after the beginning of the test. The results are plotted against time giving the percentage of biodegradation. Samples analysed are considered biodegradable when the biodegradation percentage is over 70% [20].

2.4. Experiment set-up

2.4.1. Photoreactor

Photo-Fenton experiments were carried out under sunlight in a pilot plant specially developed for photo-Fenton applications installed at Plataforma Solar de Almería (PSA, Almería, Spain). This solar reactor is composed of a continuously stirred tank, a centrifugal pump (1.5 m³ h⁻¹), a solar collector and connecting tubing and valves. The total reactor volume of 75 L is composed of two parts: 44.6 L (glass tubes) corresponding to the total irradiated volume (V_i), and the dead reactor volume (tank + tubes). The solar collector is made up of four Compound Parabolic Collector units (1.04 m² each one), mounted on an aluminium frame fixed on a south-facing platform tilted at the local latitude (37°). Each collector unit is provided by five 50 mm outer diameter borosilicate-glass tubes connected by plastic joints. A flow diagram is shown in Fig. 1.

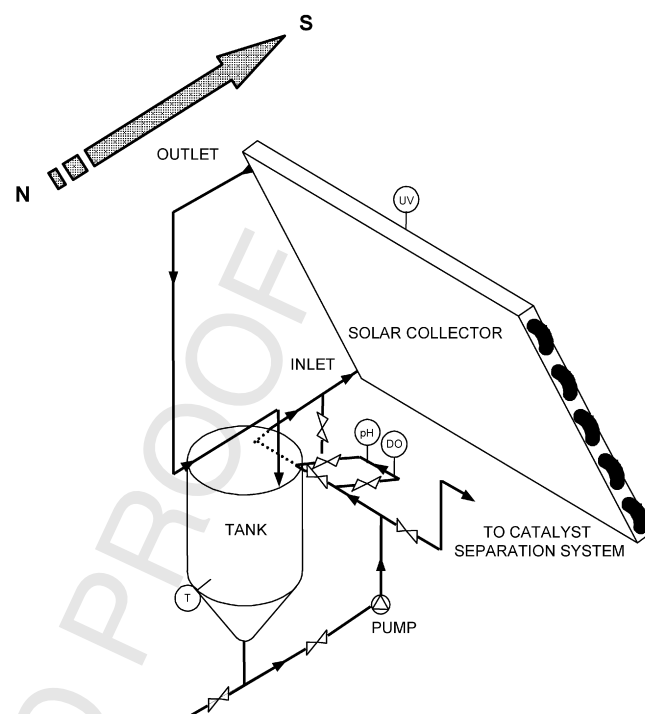


Fig. 1. Flow diagram of the photoreactor (photo-Fenton).

The pilot plant is outdoors, but a temperature control system keeps the temperature at a set point of 30 °C. Details of the pilot plant have been published elsewhere [21].

Solar ultraviolet radiation (UV) was measured by a global UV radiometer (KIPP&ZONEN, model CUV 3), mounted on a platform tilted 37°, which provides data in terms of incident $W_{UV} \text{ m}^{-2}$. In this way, the energy reaching any surface is measured in the same position with regard to the sun. With Eq. (1), combination of the data from several days' experiments and their comparison with other photocatalytic experiments is possible.

$$t_{30W,n} = t_{30W,n-1} + \Delta t_n \frac{UV}{30} \frac{V_i}{V_T}; \quad \Delta t_n = t_n - t_{n-1} \quad (1)$$

where t_n is the experimental time for each sample, UV is the average solar ultraviolet radiation measured during Δt_n , and t_{30W} is a "normalized illumination time". In this case, time refers to a constant solar UV power of 30 W m⁻² (typical solar UV power on a perfectly sunny day around noon).

At the beginning of all the photo-Fenton experiments, with the collectors covered and the reactor filled with distilled water, MPG was directly added to the photoreactor, and a sample was taken after 15 min of homogenisation (initial concentration). In the case of experiments with simulated seawater, 35 g L⁻¹ of NaCl was added and homogenized well before adding MPG. Then the pH was adjusted between 2.8 and 2.9 with sulphuric acid in order to avoid iron hydroxide precipitation and another sample was taken after 15 min to confirm the pH. Afterwards, iron salt was also added ($\text{FeSO}_4 \cdot 7\text{H}_2\text{O}$, 2 or 20 mg L⁻¹ of Fe^{2+} , Point 1) and homogenised well for 15 min before a sample was taken. Finally an initial dose of hydrogen peroxide was added (100 mL, point 2) and different samples were taken to evaluate

239 any effect in the dark, mainly the Fenton process. At that
240 moment collectors were uncovered and photo-Fenton began.
241 The concentration of peroxide in the reactor had to be kept
242 in the range of 200–500 mg L⁻¹ throughout the process, so
243 hydrogen peroxide was frequently analysed off-line and manu-
244 ally controlled to avoid complete disappearance by adding
245 small amounts as consumed.
246

247 2.4.2. Biological reactor system

248 The biological reactor erected for combined-system
249 experiments at the PSA is composed of three modules: a
250 165-L conic neutralisation tank, a 100 L conic conditioner tank
251 and a 170 L aerobic immobilised biomass reactor (IBR). A flow
252 diagram of the pilot system is shown in Fig. 2. The conditioner
253 tank is equipped with a pH control unit (CRISON, electrode and
254 pH28 controller) for pH adjustment using either H₂SO₄ or
255 NaOH dosed by means of two peristaltic pumps (ALLDOS).
256 The IBR is a flat bottom container filled with 90–95 L of
257 propylene Pall® Ring supports (nominal diameter: 15 mm,
258 density: 80 kg m⁻³, specific area: 350 m² m⁻³, void fraction:
259 0.9 m³ m⁻³), colonized by activated sludge from the municipal
260 waste water treatment plant in Almería. This bioreactor is
261 also equipped with an air blower to supply oxygen to the
262 micro-organisms, and a dissolved oxygen (DO) control unit
263 (CRISON, electrode and OXI49 controller) for maintaining
264 oxygen in the system between 4 and 6 mg L⁻¹.

265 All the experiments performed in this biological system
266 were carried out in batch mode operation. MPG waste water
267 pre-treated by photo-Fenton was pumped into the neutralisation
268 tank, where pH was neutralised by NaOH to a pH around 7.
269 This favoured catalyst (Fe²⁺) settling and separation when
270 necessary. Following this preliminary step, the photo-pretreated

effluent was piped to the conditioner tank by means of a
271 centrifugal pump, where the pH was lightly controlled in a
272 range of 6.5–7.5. Afterwards, the effluent was pumped through
273 the IBR which operated as an up-flow reactor, at a recirculation
274 flow rate of 8 L min⁻¹ between the conditioner tank and
275 the IBR, until the decreased in TOC reached characteristic
276 biological system values (20–30 mg L⁻¹). At that moment
277 combined-system treatment of the effluent could be considered
278 complete.
279

280 3. Results and discussion

281 Photodegradation of MPG dissolved in distilled water was
282 evaluated by two photo-Fenton experiments performed with
283 two different catalyst concentrations, 2 and 20 mg L⁻¹ of Fe²⁺.
284 Their comparison made it possible to select optimal photo-
285 catalytic conditions for testing the integrated system. It is worth
286 mentioning that heterogeneous photocatalysis with TiO₂ has
287 been demonstrated, as reported in previous publications, to be
288 less efficient than homogeneous photocatalysis by photo-
289 Fenton for treating this type of waste water [21]. On the other
290 hand, photo-Fenton at 20 mg L⁻¹ of Fe²⁺ has previously been
291 found optimum for the specially designed solar photoreactor
292 used in this work, not only from the point of view of degrading
293 specific contaminants [22], but also from the point of view of
294 the solar photoreactor optical behaviour [23]. In any case, as
295 the purpose of our work was to evaluate the feasibility of
296 integrating a photoreactor and a biological system, photo-
297 Fenton also was tested with only 2 mg L⁻¹ of Fe²⁺ to determine
298 whether waste water biocompatibility could be reached in a
299 reasonable length of time, as low iron concentrations are
300 enough for the photocatalytic pre-treatment step.

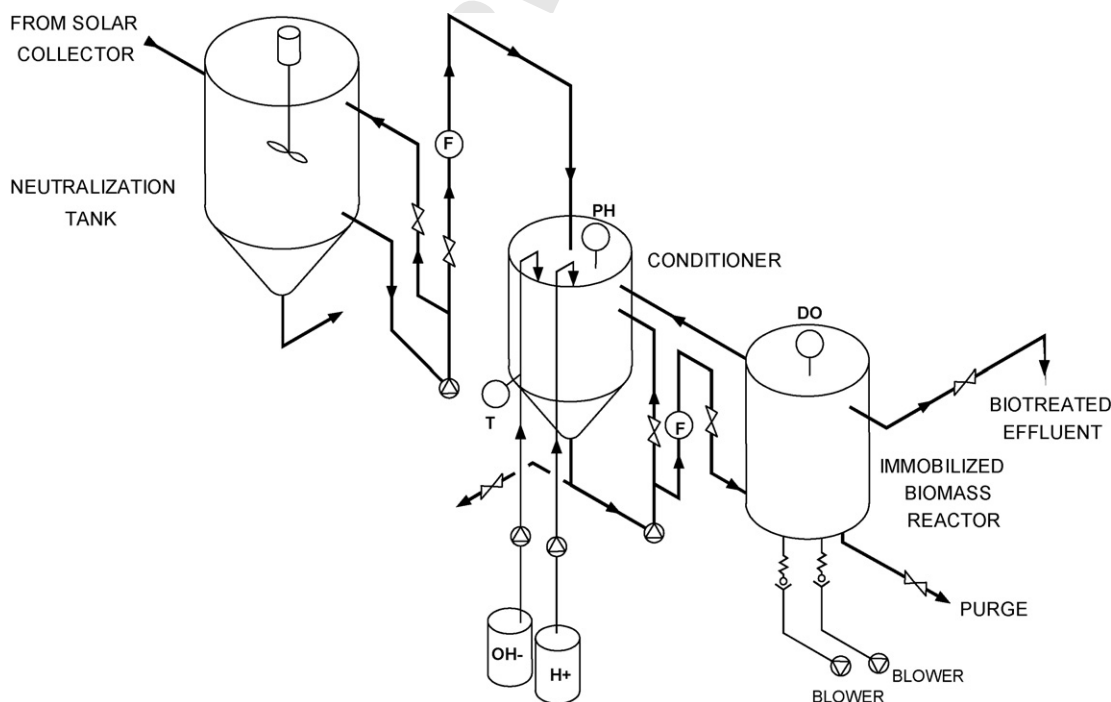


Fig. 2. Flow diagram of the biological reactor system.

All the experiments were carried out at the same MPG concentration of around 530 mg L^{-1} . All the experiments were performed at the same initial concentration of MPG, selected because the main purpose of the work was to assess whether it was possible to achieve biodegradability by photo-Fenton. This means converting MPG (known to be non-biodegradable) into other biodegradable organic compounds. As clearly shown in the results, when MPG has disappeared, considerable mineralization has been attained. Under these circumstances, it was necessary to perform tests at a high enough initial concentration for the Z–W test, as Directive 88/302/EEC recommends testing at $400 \text{ mg/L} > \text{TOC} > 50 \text{ mg/L}$ to evaluate properly the biodegradability. The mass balance of the treatment of this compound by photo-Fenton process is based on Eq. (4), where the combination of the mineralization reaction (Eq. (2)) and the decomposition of hydrogen peroxide (Eq. (3)) are considered:

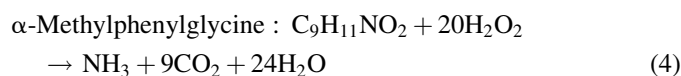
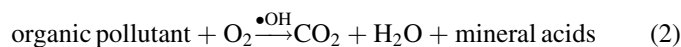


Fig. 3a, shows the degradation and mineralization of MPG during both photo-Fenton processes, as well as the hydrogen peroxide consumption corresponding to each test. It can be observed that when 20 mg L^{-1} of Fe^{2+} was employed, mineralization was almost complete (97% decrease in TOC), while using a smaller amount of catalyst (2 mg L^{-1}), the treatment time necessary for the same mineralization percentage appeared to be several times longer.

Furthermore, the significant compound degradation attained during “dark Fenton” (with the collectors covered, from point 2 to $t_{30 \text{ W}} = 0$), in both photo-Fenton tests, although it was much

more pronounced with the higher catalyst concentration (20 mg L^{-1}) is worthy of mention.

Kinetic studies of these two photo-Fenton processes were performed to support these results. Assuming that the reaction between the $\bullet\text{OH}$ radicals and the pollutant is the rate-determining step, MPG degradation may be described as a first-order reaction (Eq. (5)):

$$r = k_{\text{OH}}[\bullet\text{OH}]C = k_{\text{ap}}C \quad (5)$$

where C is the MPG concentration, k_{OH} the reaction rate constant and k_{ap} is a pseudo first-order constant. This was confirmed by the linear behaviour of $\ln(C_0/C)$ as a function of $t_{30 \text{ W}}$, for both tests performed (see Table 1).

An appreciable difference between photo-Fenton experiments performed at the two iron concentrations (around eight times faster with 20 mg L^{-1} of Fe^{2+}), was clearly observed (see Table 1) not only with regard to the required treatment time, but also to the kinetics rate constant (k_{ap}), and initial reaction rate (r_0). However, at the beginning of the process TOC mineralization was slow until at $t_{30 \text{ W}} = 20 \text{ min}$ (for $\text{Fe}^{2+} = 20 \text{ mg L}^{-1}$) and $t_{30 \text{ W}} = 115 \text{ min}$ (for $\text{Fe}^{2+} = 2 \text{ mg L}^{-1}$), when mineralization rate increased considerably. This effect could be explained by the partial MPG oxidation at the beginning of both treatments and the later complete oxidation of the intermediates generated to CO_2 , and/or the formation of more efficient iron-carboxylic complexes (hydrogen peroxide consumption was also accelerated at those points), as described below.

Hydrogen peroxide consumption was very similar (around 40 mM) for both photo-treatments until 50% of the initial TOC was eliminated (i.e., $\text{TOC} \approx 175 \text{ mg/L}$). These experiments were performed with an excess of H_2O_2 , so the drawback of the hydrogen peroxide self-decomposition reaction must be taken into consideration (Eq. (3)). The incorporation of the dissolved oxygen (from atmosphere and hydrogen peroxide decomposi-

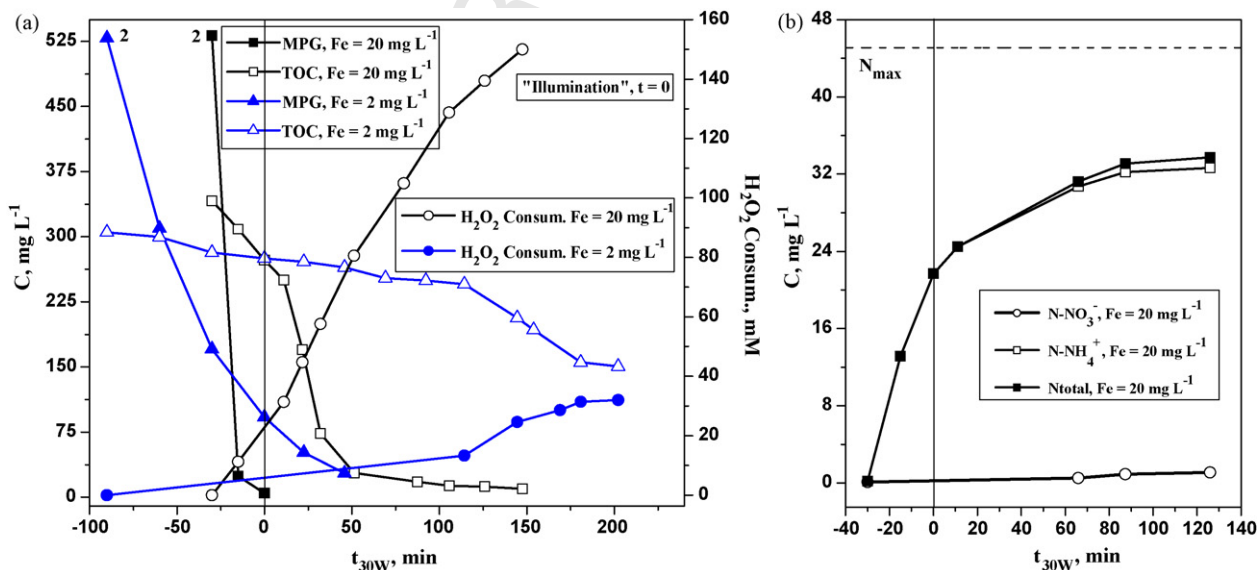


Fig. 3. (a) MPG degradation and mineralization by photo-Fenton at 2 and 20 mg L^{-1} of Fe^{2+} with distilled water. Point 2 refers to the first addition of Fe^{2+} of H_2O_2 (see Section 2.4 for details). (b) Inorganic ions released during photo-Fenton at 20 mg L^{-1} of Fe^{2+} .

Table 1
Kinetic parameters and consumption of hydrogen peroxide to eliminate approximately 50% of initial TOC

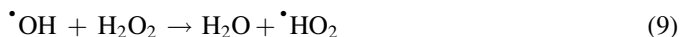
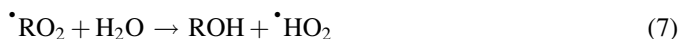
MPG	$t_{30\text{ w},50}^a$ (min)	k_{ap} (min^{-1})	R^2	r_0^b ($\text{mg L}^{-1} \text{min}^{-1}$)	$\text{H}_2\text{O}_2\text{CONS}^c$ (mM)
$\text{Fe} = 2 \text{ mg L}^{-1}$	202	0.019	0.999	10.26	32
$\text{Fe} = 20 \text{ mg L}^{-1}$	22	0.158	0.971	84.01	45

^a Treatment time necessary to eliminate approximately 50% of initial TOC.

^b Initial degradation rate from the beginning of the process to $t_{30\text{ w}} = 0$ min ($t_{\text{total}} = 30$ min for 20 mg L^{-1} and $t_{\text{total}} = 90$ min for 2 mg L^{-1}).

^c Amount of hydrogen peroxide consumed to eliminate approximately 50% of initial TOC.

tion) in the reaction mechanism by Eqs. (6) and (7) produces a peroxy radical, which can then further participate in the reaction mechanism, generating an additional hydrogen peroxide molecule (Eq. (8)). When MPG degradation proceeds, the ratio of hydrogen peroxide to pollutant increased and the reaction of the radicals generated with hydrogen peroxide (Eq. (9)) were favoured, leading to the much less reactive $\cdot\text{HO}_2$ [30]:



Depending on the ligands, the ferric iron complex has different light adsorption properties and reactions have different quantum yields at different wavelengths. Consequently, pH plays a crucial role in the efficiency of the photo-Fenton reaction, because it strongly influences which complexes are formed, this is why the pH of 2.8 was frequently postulated as optimum for photo-Fenton treatment [24,25]. At this pH, there is still no precipitation, and the dominant iron species in solution is $[\text{Fe}(\text{OH})]^{2+}$, which is the most photoactive ferric iron–water complex [26].

In fact, ferric iron can form complexes with many substances and undergo photoreduction. Of special importance are carboxylic acids because they are frequent intermediates during the last stages of an oxidative treatment. Such ferric iron–carboxylate complexes can have much higher quantum yields than ferric iron–water complexes. Therefore, the reaction typically shows an initial lag phase, until intermediates which can regenerate ferrous iron more efficiently are formed, accelerating the process.

Because of the low solubility of ferric iron hydroxide ($K_s \approx 10^{-37}$), precipitation starts at pH 2.5–3.5, depending on the iron concentration and temperature. The precipitation process starts with the formation of dimers and oligomers, which then gradually further polymerise, and lose water until finally forming insoluble iron hydroxides (e.g., goethite or hematite). This ageing process is slow [27,28], but precipitation and ageing processes are also temperature dependent. Higher temperatures yield to faster and higher precipitation of the monomer content [29] (no significant change detected during 1 day at 4°C but a decrease of the 4% was observed at 28°C). The tests reported here were performed at higher temperatures (30°C) than those described by Krýsová et al. [29], and

therefore, most of the initial Fe^{2+} (2 mg L^{-1}) may have been lost after 2–3 h of photo-treatment.

Ammonium and nitrate ions release from the initial MPG molecule were measured in different relative concentrations during the photo-Fenton ($\text{Fe}^{2+} = 20 \text{ mg L}^{-1}$) experiment (Fig. 3b). N_{total} is the combination of total nitrogen released as ammonia and nitrate from MPG degradation, which present a molar ratio of $\text{NH}_4^+/\text{NO}_3^- = 28$ at the end of the process ($t_{30\text{ w}} = 212$ min). This ratio changed during photo-treatment, since at shorter treatment times the organic nitrogen was released as ammonia and high NH_4^+ concentrations were detected, but afterwards it was slowly transformed into nitrate at the end of the process. However, the nitrogen mass balance was incomplete, as only 77% of the theoretical amount appeared after almost complete mineralization. Other researchers [31] have found that the fate of nitrogen in photocatalytic systems depends on the initial oxidation state. When present in the -3 state, as in amino groups (the case of MPG), nitrogen spontaneously evolves as NH_4^+ cations with the same oxidation state (Eqs. (10) and (11)), before being slowly oxidized into nitrate. This is exactly what was observed in the photo-Fenton treatment of MPG.



From these tests, it can be concluded that photo-Fenton treatment appears to be much more effective with 20 mg L^{-1} of Fe^{2+} than with only 2 mg L^{-1} , especially when the organic charge of the waste water was in the range of hundreds of mg L^{-1} , making photo-Fenton treatment times longer. For coupling with biological treatment, it would not be necessary to settle and separate the catalyst, since a concentration of 20 mg L^{-1} is still low enough to ensure non-inhibitory effects.

The main purpose of this work was to find out whether it was possible to enhance MPG biodegradability by an oxidative photo-Fenton pre-treatment for disposal in an aerobic biological process. Therefore, taking previous studies into account [12], different stages of photo-Fenton treatment were selected as a reference for evaluating waste water biocompatibility. In Fig. 4a, degradation and mineralization of MPG by photo-Fenton (at 20 mg L^{-1} of Fe^{2+}), is shown against treatment time. In this case an H_2O_2 limiting concentration (around 100 mg L^{-1}) was maintained during the whole process to minimize hydrogen peroxide consumption and for optimal Z–W biodegradability analysis conditions (little H_2O_2 to avoid toxic effect). While the theoretical hydrogen peroxide consumption for complete degradation of 530 mg L^{-1} of MPG (as calculated

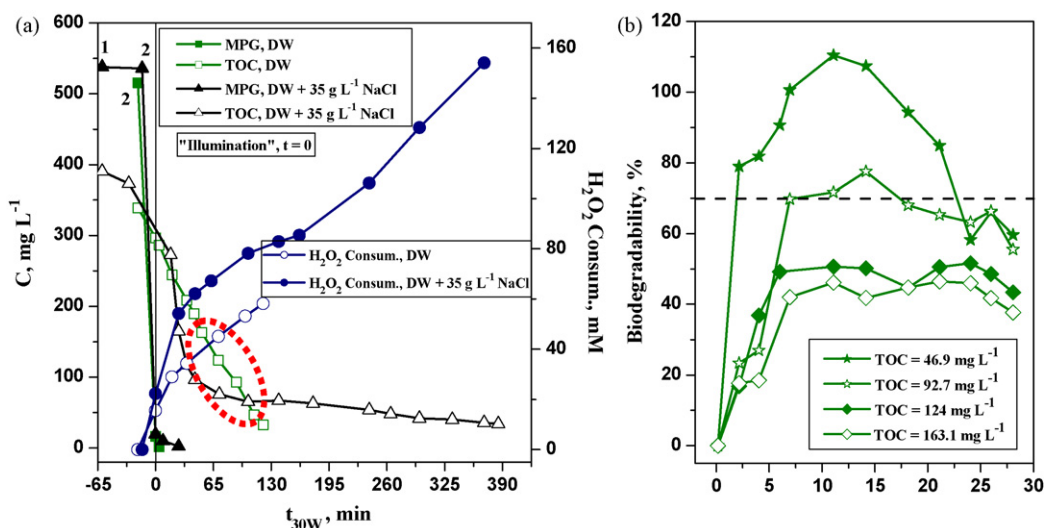


Fig. 4. (a) MPG degradation and mineralization by photo-Fenton ($\text{Fe} = 20 \text{ mg L}^{-1}$), with limited additions of H_2O_2 . Point 1 refers to the addition of the catalyst and point 2 to the first addition of H_2O_2 (see Section 2.4 for details). The surrounded part corresponds to the four samples selected for Z–W. (b) Zahn–Wellens test applied to the samples marked in (a).

460

by Eq. (4) is 64 mM, the one obtained by minimizing hydrogen peroxide consumption during the photo-Fenton treatment was lower (58 mM), this would mean a significant reduction in the corresponding operating costs. Concerning the biocompatibility analysis, a Z–W test was performed taking four pre-treated samples (marked in Fig. 4a), just after complete disappearance of MPG. These results are evaluated below.

MPG is also known to be present in industrial saline waste water, so it was considered of interest to test MPG degradation by photo-Fenton (at 20 mg L^{-1} of Fe^{2+} , minimizing H_2O_2 consumption), in simulated seawater prepared by the addition of 35 g L^{-1} of NaCl. Therefore, two experiments with manually controlled addition of hydrogen peroxide were performed, both in distilled water and in simulated seawater using 20 mg L^{-1} of catalyst (Fig. 4a).

As observed in Fig. 4a, the pollutant was also successfully degraded and mineralized (around 90% of TOC disappeared), but this time, the treatment time required for substantial mineralization of MPG was three times longer than in the previous experiment (see Fig. 3) performed with distilled water. Table 2 shows a direct comparison between the two photo-Fenton processes (at 20 mg L^{-1} of Fe^{2+}), in distilled water and simulated seawater with an H_2O_2 -limiting concentration. Kinetic studies show a similar first-order kinetic constant (k_{ap}) and initial degradation rate (r_0) in both cases, which means that no significant negative effect was found in the photo-Fenton treatment of MPG due to the characteristics of saline

water. Nevertheless, an important drawback related to the treatment time was detected when simulated seawater was employed. The treatment time necessary for 90% mineralization was around three times higher than for distilled water, leading to higher consumption of hydrogen peroxide. The effect of chloride on Fenton and photo-Fenton processes was recently reported in detail by De Laat et al. [32].

Fig. 4b, shows the percentage of biodegradability in each sample selected for the Z–W test. First of all, the pH of the samples had to be adjusted to 6.5–7.5 (optimal pH for biological systems) with NaOH, as the pH in the photo-Fenton process was around 2.8–2.9. Then, the Z–W was started and maintained properly aerated and agitated for 28 days. As observed in the figure, the percentage of biodegradability in waste water with the higher TOC (163.1 and 124 mg L^{-1}) pre-treated by photo-Fenton was only between 40 and 50%. Degradation was more pronounced in the first 5 days of biotreatment, but afterwards, no appreciable change was detected. The generation of non-biodegradable (but non-toxic) intermediates during advanced stages of the photo-Fenton treatment could be inferred from these low percentages. Biodegradability over 70% was reached in the samples with lower TOC values in both cases. Biodegradability reached 80% in the sample with $\text{TOC} = 46.9 \text{ mg L}^{-1}$ in only 2 days and continued increasing until complete biodegradation of TOC. After reaching the maximum, it decreased because of the cell's death (no feed was available) and organic carbon was released

Table 2

Kinetic parameters and consumption of hydrogen peroxide to eliminate 90% of the initial TOC, when MPG was dissolved in distilled water and in simulated seawater

MPG	$t_{30 \text{ W}, 90}^{\text{a}}$ (min)	k_{ap} (min^{-1})	R^2	r_0^{b} ($\text{mg L}^{-1} \text{ min}^{-1}$)	$\text{H}_2\text{O}_{2\text{CONS}}^{\text{c}}$ (mM)
$\text{Fe} = 20 \text{ mg L}^{-1}$	121	0.219	0.939	112.83	58
$\text{Fe} = 20 \text{ mg L}^{-1} + 35 \text{ g L}^{-1} \text{ NaCl}$	385	0.176	0.959	94.74	154

^a Treatment time necessary to eliminate approximately 90% of initial TOC.

^b Initial degradation rate from the beginning of the process to $t_{30 \text{ W}} = 0$ for $20 \text{ mg L}^{-1} + \text{NaCl}$ ($t_{\text{total}} = 60 \text{ min}$) and to $t_{30 \text{ W}} = 4.2 \text{ min}$ for 20 mg L^{-1} ($t_{\text{total}} = 60 \text{ min}$).

^c Amount of hydrogen peroxide consumed to eliminate approximately 90% of initial TOC.

514 from the inside of the cells. On the other hand, the sample with
515 TOC = 92.7 mg L⁻¹, reached only 70% biodegradability in
516 around 5 days and remained the same for the rest of the Z–W
517 test. Samples with a biodegradability of 70% are already
518 considered biodegradable, so the best point for discharging the
519 photo-Fenton effluent to an aerobic biological system could be
520 established as just when MPG was completely degraded and the
521 TOC decreased to around 90–95 mg L⁻¹.

522 In this sense, the integrated system was better for total
523 mineralization of the photo-treated solution, since using the
524 photo-Fenton reactor alone is not economically attractive for
525 reaching satisfactory mineralization levels. For example, an
526 increase of the operating costs (mainly as hydrogen peroxide
527 consumption) of approximately 20% could be considered
528 when photo-Fenton reactor is used alone. Moreover, the
529 general investment increase (m² of collectors field needed for
530 total mineralization), could be estimated in approximately
531 50%.

532 Taking into account previous similar studies [12,13] and the
533 results above, several batch photo-Fenton experiments were
534 performed (at 20 mg L⁻¹ of Fe²⁺) until complete degradation of
535 MPG and a corresponding TOC of around 95 mg L⁻¹, to
536 provide enough photo-treated water to the biological reactor.
537 First of all, the immobilised biomass reactor was inoculated
538 with 150 L of activated sludge from a municipal waste water
539 treatment plant, and recirculated between the conditioner tank
540 and the IBR for nearly 2 weeks in order to ensure optimal
541 fixation of the sludge on the polypropylene supports. The total
542 suspended solids, TOC and inorganic ions concentration
543 (mainly ammonia and nitrate) were measured daily.

544 The analysis of total suspended solids (TSS) was used to
545 assess bacteria fixation on the supports during IBR inoculation,
546 a variation from 0.42 g L⁻¹ to 0 in approximately 10 days was
547 detected. That is when the IBR could be considered in adequate
548 condition for the biological treatment of waste water from the
549 photo-Fenton pre-oxidation process.

550 Afterwards, the solution pre-treated with photo-Fenton
551 flowed directly into the neutralisation tank of the biological
552 system and following the procedure explained in Section 2.4
553 (biological reactor system), the pH was adjusted roughly to 7.
554 Only a few grams per batch of iron sludge were produced
555 because of the low concentration of iron. Then the effluent was
556 pumped to the conditioner tank, where pH was kept between
557 6.5 and 7.5, and dissolved oxygen between 4 and 6 mg L⁻¹. The
558 mineral medium specified in the Z–W test protocol to ensure
559 proper metabolic activity of the bacteria, was also added
560 considering the ammonia concentration already present in the
561 photo-treated effluent. The biological system was operated in
562 batch mode and recirculated between the conditioner tank and
563 the IBR until the solution TOC remained constant from around
564 20 to 30 mg L⁻¹, which characteristically correspond to
565 background noise from the physiological bacteria activity
566 found in conventional biological media. Total mineralization
567 was therefore impossible (TOC below 20 mg L⁻¹) in this
568 biological degradation system.

569 Fig. 5 shows the evolution of TOC in both photochemical
570 and biological treatments. It may be observed that the solar
571 system was able to remove 76% of the TOC from an initial load
572 of 430 mg L⁻¹ after 3.5 h of photo-oxidation. Then the pre-
573 treated solution was discharged to the biological process where
574 complete mineralization was achieved in around 3 days,
575 indicating that the photo-pretreatment was able to produce a
576 biocompatible solution. The global efficiency of this combined
577 system was 95% removal of the initial TOC. Fig. 5 also shows
578 the TOC from MPG only. This was calculated by taking the
579 MPG concentration measured by HPLC and transforming it
580 into TOC values. Total elimination of the pollutant before the
581 pre-treated effluent was discharged to the biological system was
582 clearly demonstrated.

583 Ammonia and nitrate concentrations were also measured
584 during the biological process and plotted against treatment time
585 (see Fig. 5). As it may be observed, nitrification was detected
586

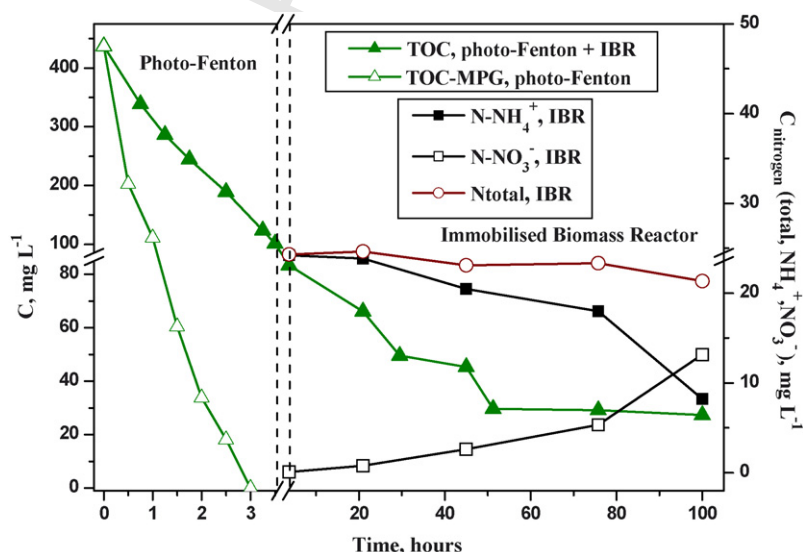
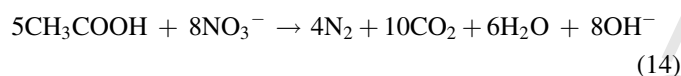
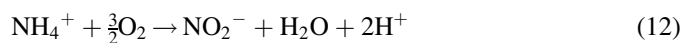


Fig. 5. MPG degradation and mineralization by the combined system. Inorganic ions measured in the immobilised biomass reactor are also shown.

during biotreatment (Eqs. (12) and (13)), meaning that nitrification bacteria consumed the nitrogen from NH_4^+ for its metabolic activity, and transformed it into NO_3^- , which was excreted to the media. A decrease in nitrogen concentration from NH_4^+ of around 16.0 mg L^{-1} (corresponding to 20.6 mg L^{-1} of ammonium), was measured, while the nitrogen concentration from NO_3^- , increased to around 13.1 mg L^{-1} (57.9 mg L^{-1} of nitrate). Nevertheless, this increase was lower than expected if all the nitrogen from ammonia had been transformed into nitrate. According to these results, there seemed to be slight denitrification in the last step of the biological process leading to disappearance of around 2.94 mg L^{-1} of total nitrogen as N_2 , and also because of an uptake by bacteria for their growth. This slight elimination of nitrogen occurred because fixed biomass systems have a dissolved oxygen deficiency in the inner wall of the biofilm fixed on the supports, due to the extremely low oxygen transfer to the inner layers of biomass. These anoxic conditions made nitrate became an electron acceptor (instead of oxygen) for organic carbon oxidation leading to N_2 generation, which was eliminated into the atmosphere (Eq. (14), where HOAc corresponds to a carbon source, for example acetate).



Denitrification only appeared at the end of the biotreatment as older biomass is required for this process. On the other hand, slight denitrification was detected in the bioreactor due to the low organic carbon source (electron donors) remaining at the end of the biological process.

4. Conclusions

It has been demonstrated that MPG dissolved in distilled water can be treated successfully by photo-Fenton in a reasonable length of time. Moreover, Photo-Fenton treatment with 20 mg L^{-1} of Fe^{2+} was efficient enough, and no catalyst separation was required in the combined system, as the concentration was low enough to ensure non-inhibitory effects on the activated sludge. Photo-Fenton (at 20 mg L^{-1}) in simulated seawater was also found to have been successful, but with longer treatment times than for distilled water.

Evaluation of the combined photocatalytic-biological system developed has demonstrated that in batch mode operation, photo-Fenton pre-treatment completely removed the pollutant (MPG) and enhanced its biodegradability, producing a biocompatible effluent which was completely mineralized by the biological system in an immobilised biomass reactor. The combined system was able to totally mineralize 95% of initial TOC of over 400 mg L^{-1} .

The beneficial effects of this two-steps field treatment has therefore been confirmed at pilot scale. Photo-Fenton under sunlight using CPC reactors was able to remove the bio-

recalcitrant compound and produce biocompatible intermediates required for further biological treatment. These results indicate that a combined solar photocatalytic-biological process is an effective approach for the treatment of biorecalcitrant pollutants present in water.

Acknowledgements

The authors wish to thank the European Commission for its financial support under the CADOX project (Contract. No. EVK1-CT-2002-00122). The valuable collaboration of the Almerías Waste water Treatment Plant (Mr. Eduardo Ruiz, AQUALIA) is much appreciated. They also wish to thank Mrs. Deborah Fuldauer for correcting the English. Isabel Oller would like to thank the Spanish Ministry of Education and Science for her Ph.D. research grant.

References

- [1] P.R. Gogate, A.B. Pandit, *Adv. Environ. Res.* 8 (2004) 501.
- [2] P.R. Gogate, A.B. Pandit, *Adv. Environ. Res.* 8 (2004) 553.
- [3] A. Safarzadeh-Amiri, J.R. Bolton, S.R. Cater, *J. Adv. Oxid. Technol.* 1 (1996) 18.
- [4] C. Pulgarín, M. Invernizzi, S. Parra, V. Sarria, R. Polania, P. Péringier, *Catal. Today* 54 (1999) 341.
- [5] D. Bahnemann, *Sol. Energy* 77 (2004) 445.
- [6] S. Malato, J. Blanco, A. Vidal, C. Ritcher, *Appl. Catal. B: Environ.* 37 (2002) 1.
- [7] A. Marco, S. Espugas, G. Saum, *Water Sci. Technol.* 35 (1997) 321.
- [8] J.P. Scott, D.F. Ollis, *Environ. Progress* 14 (1995) 88.
- [9] J.P. Scott, D.F. Ollis, *J. Environ. Eng.* 122 (1996) 1110.
- [10] S. Parra, S. Malato, C. Pulgarín, *Appl. Catal. B: Environ.* 36 (2002) 131.
- [11] M. Rodríguez, V. Sarria, S. Espugas, C. Pulgarín, *J. Photochem. Photobiol. A: Chem.* 151 (2002) 129.
- [12] V. Sarria, S. Parra, N. Alder, P. Péringier, N. Benitez, C. Pulgarín, *Catal. Today* 76 (2002) 301.
- [13] V. Sarria, S. Kenfack, O. Guilled, C. Pulgarín, *J. Photochem. Photobiol. A: Chem.* 159 (2003) 89.
- [14] V. Sarria, M. Deront, P. Péringier, C. Pulgarín, *Appl. Catal. B: Environ.* 40 (2003) 231.
- [15] S. Contreras, M. Rodríguez, F. AlMomani, C. Sans, S. Espugas, *Water Res.* 37 (2003) 3169.
- [16] M. Bressan, L. Liberatore, N. D'Alessandro, L. Tonucci, C. Belli, G. Ranalli, *J. Agric. Food Chem.* 52 (2004) 1228.
- [17] EC, Implementation of Council Directive 91/27/EEC of 21 May 1991 concerning urban waste water treatment, as amended by Commission Directive 98/15/EC of 27 February 1998, Commission of the European Communities, COM (2004) 248 final, Brussels, 2004.
- [18] R. Maciel, G.L. Sant'Anna, M. Dezotti, *Chemosphere* 57 (2004) 711.
- [19] J.E.F. Moraes, F.H. Quina, C.A.O. Nascimento, D.N. Silva, O. Chiavone-Filho, *Environ. Sci. Technol.* 38 (2004) 1183.
- [20] M. Lapertot, C. Pulgarín, *Water Res.*, in press.
- [21] I. Oller, P. Fernández-Ibáñez, M.I. Maldonado, L. Pérez-Estrada, W. Gernjak, C. Pulgarín, P.C. Passarinho, S. Malato, *Res. Chem. Interm.*, in press.
- [22] M. Hincapié Pérez, G. Peñuela, M.I. Maldonado, P. Fernández-Ibáñez, I. Oller, W. Gernjak and S. Malato, *Appl. Catal. B: Environ.*, in press.
- [23] S. Malato Rodríguez, J. Blanco Gálvez, M.I. Maldonado Rubio, P. Fernández Ibáñez, D. Alarcón Padilla, M. Collares Pereira, J. Farinha Mendes, J. Correia de Oliveira, *Sol. Energy* 77 (2004) 513.
- [24] A. Safarzadeh-Amiri, J.R. Bolton, S.R. Cater, *J. Adv. Oxid. Technol.* 1 (1996) 18.
- [25] J.J. Pignatello, *Environ. Sci. Technol.* 26 (1992) 944.

- | | | | |
|-----|---|---|-----|
| 700 | [26] J.J. Pignatello, E. Oliveros, A. MacKay, <i>Crit. Rev. Environ. Sci. Technol.</i> 36 (2006) 1. | [30] W. Gernjak, M. Fuerhacker, P. Fernández-Ibáñez, J. Blanco, S. Malato, <i>Appl. Catal. B: Environ.</i> 64 (2006) 121. | 705 |
| 701 | | | 706 |
| 702 | [27] C.M. Flynn Jr., <i>Chem. Rev.</i> 84 (1984) 31. | [31] H. Lachheb, E. Puzenat, A. Houas, M. Ksibi, E. Elaloui, C. Guillard, J.M. Herrmann, <i>Appl. Catal B: Environ.</i> 39 (2002) 75. | 707 |
| 703 | [28] M. Blesa, E. Matijevic, <i>Adv. Colloid Interface Sci.</i> 29 (1989) 173. | | 708 |
| 704 | [29] H. Krýsová, J. Jirkovský, J. Krýsa, G. Mailhot, M. Bolte, <i>Appl. Catal. B: Environ.</i> 40 (2003) 1. | [32] J. De Laat, G.T. Lee, B. Legube, <i>Chemosphere</i> 455 (2004) 715. | 709 |
| 705 | | | 710 |

UNCORRECTED PROOF